FOURTH TECHNICAL PROGRESS REPORT
JULY, 1995
ON

HYDRODYNAMIC MODELS FOR SLURRY BUBBLE COLUMN REACTORS

D.Gidaspow, Principal Investigator
Department of Chemical Engineering
Illinois Institute of Technology
Chicago, Illinois 60616

ABSTRACT

The objective of this investigation is to convert our "learning gas-solid-liquid" fluidization model into a predictive design model. The IIT hydrodynamic model computes the phase velocities and the volume fractions of gas, liquid and particulate phases. Model verification involves a comparison of these computed velocities and volume fractions to experimental values.

This report includes the paper submitted for presentation at the U.S. Department of Energy 1995 Coal Liquefaction and Gas Conversion Contractors Review Meeting to be held in Pittsburgh, August 29--31, 1995. This paper was sent to P. Z. ZHOU for preprinting.

The simulations of Air Products methanol reactors described in this paper are continuing . Granular temperatures and viscosities have been computed. Preliminary measurements of granular temperatures using the Air Products catalysts were obtained using our CCD camera.

"U.S. DOE PATENT CLEARANCE NOT REQUIRED PRIOR TO PUBLICATION OF THIS REPORT."

DISCLAIMER

TITLE: HYDRODYNAMIC MODELS FOR
SLURRY BUBBLE COLUMN REACTORS

PI: Dimitri Gidaspow

STUDENT(s) Mitra Bahary, Ph.D. December 1994 and
Yuangxiang Wu, Ph.D. Candidate

INSTITUTION: Illinois Institute of Technology
Department of Chemical Engineering
IIT Center
Chicago, IL 60616
(312) 567-3045

GRANT NO. DE-FG22-94PC94208

PERIOD OF PERFORMANCE: June 1994 to June 1995

OBJECTIVE: The objective of this investigation is to convert our "learning gas-solid-liquid" fluidization model into a predictive design model. This model is capable of predicting local gas, liquid and solids hold-ups and the basic flow regimes: the uniform bubbling, the industrially practical churn-turbulent (bubble coalescence) and the slugging regimes. Current reactor models incorrectly assume that the gas and the particle hold-ups (volume fractions) are uniform in the reactor. They must be given in terms of empirical correlations determined under conditions that radically differ from reactor operation. In the proposed hydrodynamic approach these hold-ups are computed from separate phase momentum balances. Furthermore, the kinetic theory approach computes the high slurry viscosities from collisions of the catalyst particles. Thus particle rheology is not an input into the model.

WORK DONE AND CONCLUSIONS:

The IIT hydrodynamic model computes the phase velocities and the volume fractions of gas, liquid, and particulate phases. Model verification involves a comparison of these computed velocities and volume fractions to experimental values.

- A combination of X-ray and gamma-ray densitometers was used to measure the solids and the liquid volume fractions in a two dimensional bed in the bubble coalesced regime. There is a reasonable agreement between preliminary theoretical computations for an asymmetric distributor and the experiments.

- A high resolution micro-imaging/measuring system apparatus was used to measure instantaneous and time averaged particle velocities. The fluctuations of particle velocities around their average were found to be approximately Mawellian. The measured time averaged velocities compare reasonably well with the predicted velocities for an asymmetric distributor used in this study.

1

- A Brookfield viscometer was used to measure the "apparent" bed viscosity in two three-phase fluidized beds. The viscosities were also calculated from measurements of particle oscillations (granular temperature) using a high resolution micro-imaging/measuring system. To obtain these viscosities a dense phase kinetic theory formula derived in D. Gidaspow's book ("Multiphase Flow and Fluidization. Continuum and Kinetic Theory Descriptions," Academic Press, 1994) was used. There is an excellent agreement between the macroscopically measured viscosities using a Brookfield viscometer and those computed from particle fluctuations and collisions using kinetic theory.

- This comparison of viscosities computed from particle collisions and measured macroscopically and related viscosity measurements of gas-solid flow in a pipe, obtained by 3 methods, to be reported at the Miami 1995 AIChE meeting validates the proposed kinetic theory approach.

- Our computer code was modified to include reactions. A numerical simulation of synthesis of methanol in a G-L-S slurry reactor based on Air Products' LaPorte's Run E-2-B (1987) was carried on our HP700 Work-Station. We have computed the observed catalyst distribution and methanol production.

- After a discussion with DOE and Air Products representatives in late January 1994, we modified our computer code for computation with gas rather than liquid as a continuous phase to simulate Air Products RUN E-8.1 (1991). The results of this simulation presented in this paper show that the model predicts close to the experimentally observed gas-hold-up and the methanol production.

2

INTRODUCTION

Gas-liquid-solid fluidization systems are used in a variety of applications such as resid hydroprocessing, coal liquefaction or methanol production from syntheses gas in the presence of catalyst, biological wastewater treatment and fermentation (Fan, 1989). Overall three-phase fluidized bed behavior, bubble motion and breakage have been experimentally studied by a number of researchers (Fan, 1989; Kim et al., 1985; Henrickson and Ostergaard, 1974). Shah, et al. (1982) have reviewed flow regimes: bubble flow, slug flow, and churn-turbulent flow, depending on the column diameter and the superficial gas velocity. However, recent reviews by Fan (1989), Tarmy and Coulaloglou (1992) show that there exist no hydrodynamic models for three-phase fluidized beds in the literature.

In this paper a three fluid model is presented that predicts the gas, liquid and solid hold-ups (volume fractions) and flow patterns in the bubbly and in the industrially important churnturbulent (bubble coalesced) regimes. The input into the model can be either particulate viscosities as measured with a Brookfield viscometer, or derived using the mathematical techniques of kinetic theory of granular flows pioneered by Savage (1983), Jenkins and Collaborators for particulate flows without an interstitial fluid. The kinetic theory is described in three chapters in a book by Gidapow (1994).

HYDRODYNAMIC MODEL

The physical principles used are the laws of conservation of mass and momentum for the gas, the liquid and the solid phases, as shown in Table 1. The constitutive equations for the stress are shown in Table II.

COMPARISON OF COMPUTATIONS TO IIT EXPERIMENT

The hydrodynamic model was used to compute gas-liquid-solid flows in the dispersed and in the free bubbling regions (Gidapow, et al. 1994). A two dimensional bed shown in Figure 1 was constructed at IIT to operate in the dispersed flow regime. Figure 2 shows bubble coalsence in the bed and Figure 3 shows the computed time average volume fractions of 800 μm glass beads. The computations were made for an asymmetric distributor depicted in Figure 3. A combination of X-ray and gamma ray densitometers were used to obtain the hold up.

A digital camera technique was developed to measure particle velocities. It involves a measurement of a particle streak on a computer monitor for a millisecond time interval (Baha.ry, 1994). Figure 6 shows a typical measure/velocity distribution. A fit of the data to a Maxwellian or normal probability distribution gives the mean and the fluctuating velocity distributions. Figure 7 gives a comparison of these values to the computed velocities.

PARTICULATE VISCOSITY FROM KINETIC THEORY

The variance obtained from data such as depicted in Figure 6 gives the granular

temperature. Gidaspow (1994) reviews this theory. Table 3 shows a comparison of the computed viscosity using the measured granular temperature and the theoretical formula to the viscosity obtained from a Brookfield viscometer. The agreement is excellent.

REACTION MODEL

A reaction model for production of methanol using an approach similar to that described in the Vikings System (1993) report was added to the hydrodynamic computer code. The first computer run described in our first quarterly report involved a simulation of early Air Products systems in which a liquid flowed continuously through the reactor like the IIT experiment described in the previous section. Our computations agreed with Air Products methanol production. We had also computed solids hold-up that agreed with data obtained at Air Products using a nuclear gauge. Since the new Air Products design involves no liquid recirculation but is like a batch system with only gases entering and leaving the reactor, we changed our hydrodynamic model to operate with gas as a continuous phase. We simulated Run E8. of Air Products and Chemicals (1991).

Table 4 shows the reaction model. Figure 8 depicts the grid used. The obstacles shown represent heat exchangers. At this stage we assumed isothermal operation. Typical flow patterns are shown in Figure 9. Figure 10 gives the computed time average area averaged liquid, gas and solids volume fractions. The gas solid-up is close to that reported by Air Products (1991). Table 5 shows a good comparison of IIT's simulation to Air Products data for Run E8.1. Figure 11 shows the time and area averaged gas profiles along the reactor height.

ACKNOWLEDGEMENT

REFERENCES CITED:

Air Products and Chemicals, Inc., "Liquid-Entrained Catalyst Operations at LaPorte Methanol Process 1984-1985", Final Report to DOE for Contract No. DE-AC-22-81PC300019 (1987)

Air Products and Chemicals, Inc., "Liquid Phase Methanol LaPorte Process Development Unit: Modification, Operation, and Support Studies", Draft Report to DOE for Contract No. DE-AC22-87PC90005 (1991).

Air Products and Chemical, Inc., "Synthesis of Dimethyl Ether and Alternative fuels in the Liquid Phase from Coal-Derived Synthesis Gas", Topical Report to DOE for Contract No. DE-AC222-90PC89865 (1992).

Bahary, M. (1994) Experimental and Computational Studies of Hydrodynamics of Three-phase Fluidization, Ph.D Thesis, Illinois Institute of Technology, Chicago, Illinois.

Fan, L.S. (1989). Gas-Liquid-Solid Fluidization Engineering, Butterworths, Boston.

Gidaspow, D. (1994). Multiphase Flow and Fluidization. Continuum and Kinetic Theory Descriptions. Academic Press, Boston.

G.H. Graff, J.G.M. Winkelman, E. J. Stamhuis and A.A.C.M. Beenachers, "Kinetics of the Three-Phase Methanol Synthesis, "Chem. Eng. Sci., Vol. 43, No. 8, P2161-68 (1988)

Henriksen, H.K., and Ostergaard, K. (1974). On the Mechanism of Large Bubbles in Liquid and Three Phase-Fluidized Beds. Chem. Engng. Sci., 29, 626.

Hetzler and Williams, (1969). Fluidized Bed Viscosity and Expansion, Correlated With Glass Forming liquid Model, I & EC Fund., 666-677.

Jenkins, J.T., and Savage, S.B. (1983) A Theory for the Rapid Flow of Identical, Smooth, Nearly Elastic, Spherical Particles. J. Fluid Mech., 130, 187-202

Kim, S.D., Baker, C.G.J and Bergougnou, M.A. (1975). Phase Holdup Characteristics of Three Phase Fluidized Beds, Can. J. Chem Engng., 53, 134.

Savage S.B. Granular Flows at High Shear Rates. Theory of Dispersed Multiphase Flows (ed. R.E. Meyer). Academic Press, 39-358 (1983).

Seo, Y.C. and Gidaspow, D. "An x-ray gamma-ray Method of Measurement of Binary Solids Concentrations and Voids in Fluidized Beds. I & EC Research, 26 1622-1628 (1987).

Shah, Y.T., B.G. Kelkar and S.P. Godbole, "Design Parameters Estimations for Bubble Column Reactors," AIChE J. 28, 353-379 (1982).

Tamry, B.L. and C.A. Coulaloglou, "Alpha-Omega and Beyond. Industrial Veiw of Gas/Liquid/Solid Reactor Development," Chem. Eng. Science, 47, 3231-3246 (1992).

Viking Systems International Report to DOE/PETC (1993) "Design of Slurry Reactor for Indirect Liquefaction Applications."

Table 1 Conservation Equations

Continuity Equation for phase k (=g, l, s)

$$\frac{\partial}{\partial t}(\varepsilon_k \rho_k) + \nabla \cdot (\varepsilon_k \rho_k v_k) = m_k$$

Momentum Equations

(a) Gas Phase (Continuous Phase)

$$\frac{\partial}{\partial t}(\varepsilon_g \rho_g v_g) + \nabla \cdot (\varepsilon_g \rho_g v_g v_g) = -\nabla p + \rho_g g + \sum_{m=\ell,s} \beta_{gm}(v_m - v_g) + \nabla \cdot [\tau_g] + m_g v_g$$

(b) Liquid and Solid Phases k (=l, s) (Dispersed Phases)

$$\frac{\partial}{\partial t}(\varepsilon_k \rho_k v_k) + \nabla \cdot (\varepsilon_k \rho_k v_k v_k) = -\nabla P_k + \frac{\varepsilon_k}{\varepsilon_g}\left(\rho_k - \sum_{m=g,\ell,s}\varepsilon_m \rho_m\right)g$$

$$+ \sum_{m=g,\ell,s,m\neq k} \beta_{km}(v_m - v_k) + \nabla \cdot [\tau_k] + m_k v_k$$

Table 2 Drag Coefficients, Shear Stresses, Solid Pressure. k = l, s

For $\varepsilon_g < 0.8$, (based on Ergun equation)

$$\beta_{gk} = \beta_{kg} = 150\frac{(1-\varepsilon_g)\varepsilon_k \mu_g}{(\varepsilon_g d_k \psi_k)^2} + 1.75\frac{\rho_g \varepsilon_k |v_g - v_k|}{\varepsilon_g d_k \psi_k}$$

For $\varepsilon_g > 0.8$, (based on empirical correlation)

$$\beta_{gk} = \beta_{kg} = \frac{3}{4}C_D \frac{\rho_g \varepsilon_k |v_g - v_k|}{d_k \psi_k}\varepsilon_g^{-2.65}$$

$$\beta_{\ell s} = \beta_{s\ell} = \frac{3}{2}\alpha_{\ell s}(1+e)\frac{\rho_s \rho_\ell \varepsilon_s \varepsilon_\ell |v_\ell - v_s|}{\rho_s d_s^3 + \rho_\ell d_\ell^3}(d_s + d_\ell)^2$$

$$\tau_g = \varepsilon_g \mu_g\left\{[\nabla v_g + (\nabla v_g)^T] - \frac{2}{3}\nabla \cdot v_g I\right\}$$

$$\tau_k = \mu_k[\nabla v_k + (\nabla v_k)^T] - \frac{2}{3}\mu_k \nabla \cdot v_k I$$

$$\nabla P_k = G(\varepsilon_k)\nabla \varepsilon_k$$

Where

$$C_D = \begin{cases} \frac{24}{Re_k}(1 + 0.15 Re_k^{0.687}) & Re_k < 1000 \\ 0.44 & Re_k > 1000 \end{cases}$$

$$Re_k = \frac{\rho_g \varepsilon_g |v_g - v_k| d_k \psi_k}{\mu_g} \qquad e = 0.9999 \qquad \alpha_{\ell s} = 0.5$$

$$G(\varepsilon_k) = 10^{8.76\varepsilon_k - 0.27} \quad (dynes/cm^2) \qquad \mu_s = 5.0\varepsilon_s$$

6

Liquid Out

Scintillation
Detector

Gamma Ray or
X-ray Source

Intensity
Counter

Liquid Reservoir

Fiber Optic Light

Gas Distributor

Rotameter

CCD Camera

Liquid Pump

Camera Adopter

Rotameter

Multisys. Monitor

Air

PC 486
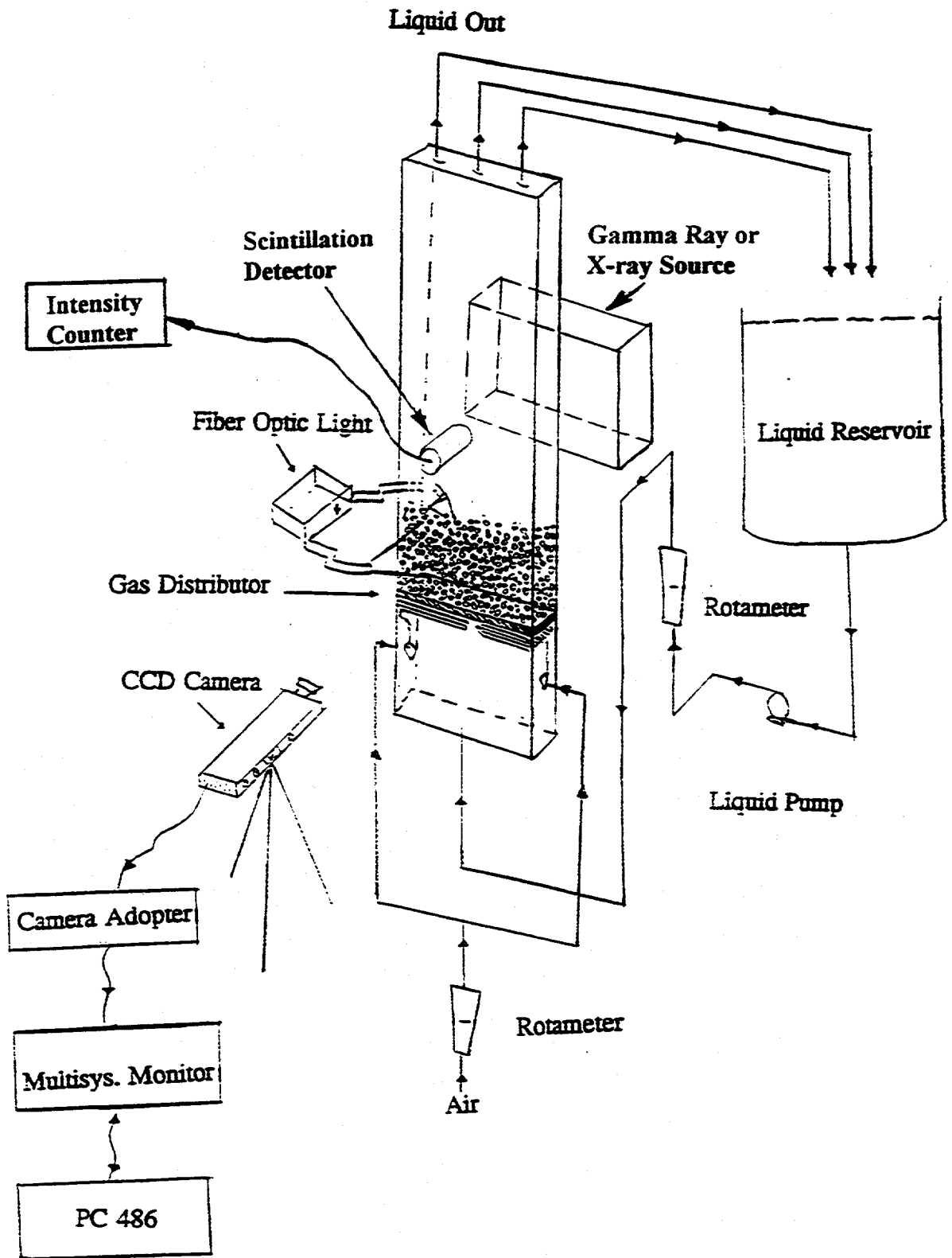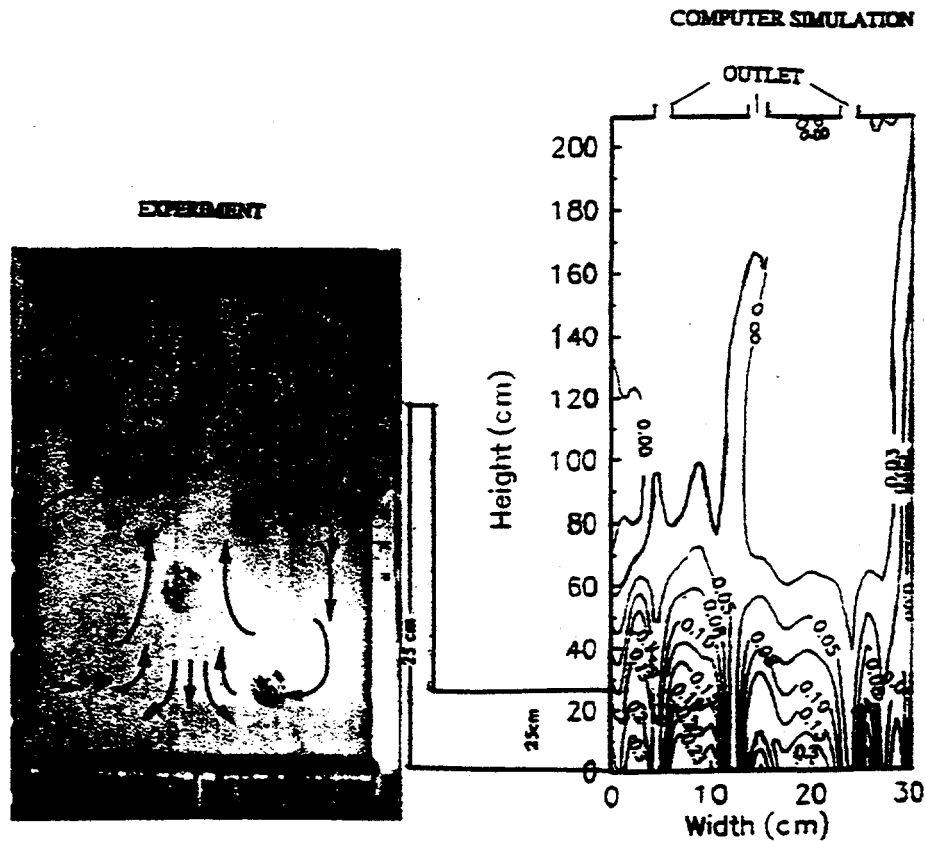
Figure 1 Three Phase 2-D Bed Apparatus at IIT

7

Table 3 Viscosity Measurements

$$\mu_s = \frac{2\mu_{dil}}{(1+e)g_0}\left[1+\frac{4}{5}(1+e)g_0\varepsilon_s\right]^2 + \frac{4}{5}\varepsilon_s^2\rho_s d_s(1+e)g_0\left(\frac{\theta_s}{\pi}\right)^{1/2}$$

where:
$$\mu_{dil} = \frac{5\sqrt{\pi}}{96}\rho_s d_s\sqrt{\theta_s} \qquad g_0 = \left[1-\left(\frac{\varepsilon_s}{\varepsilon_{s,max}}\right)^{1/3}\right]^{-1}$$

ε_s	g_0	$\theta_s(cm^2/s^2)$ Velocity Measurement	μ_s(poise) Velocity Measurement	μ_s(poise) Brookfield Viscometer
0.346	5.39	845	4.26	4.359
0.272	4.03	435	2.947	3.125

Fig. 2 Photograph of Bubble Coalescence in a G-L-S Fluidized Bed (V_g=3.37 cm/s, V_l=2.03 cm/s)

COMPUTER SIMULATION

Fig. 3 Computed Time Average Volume Fraction Contours for Solid Phase.
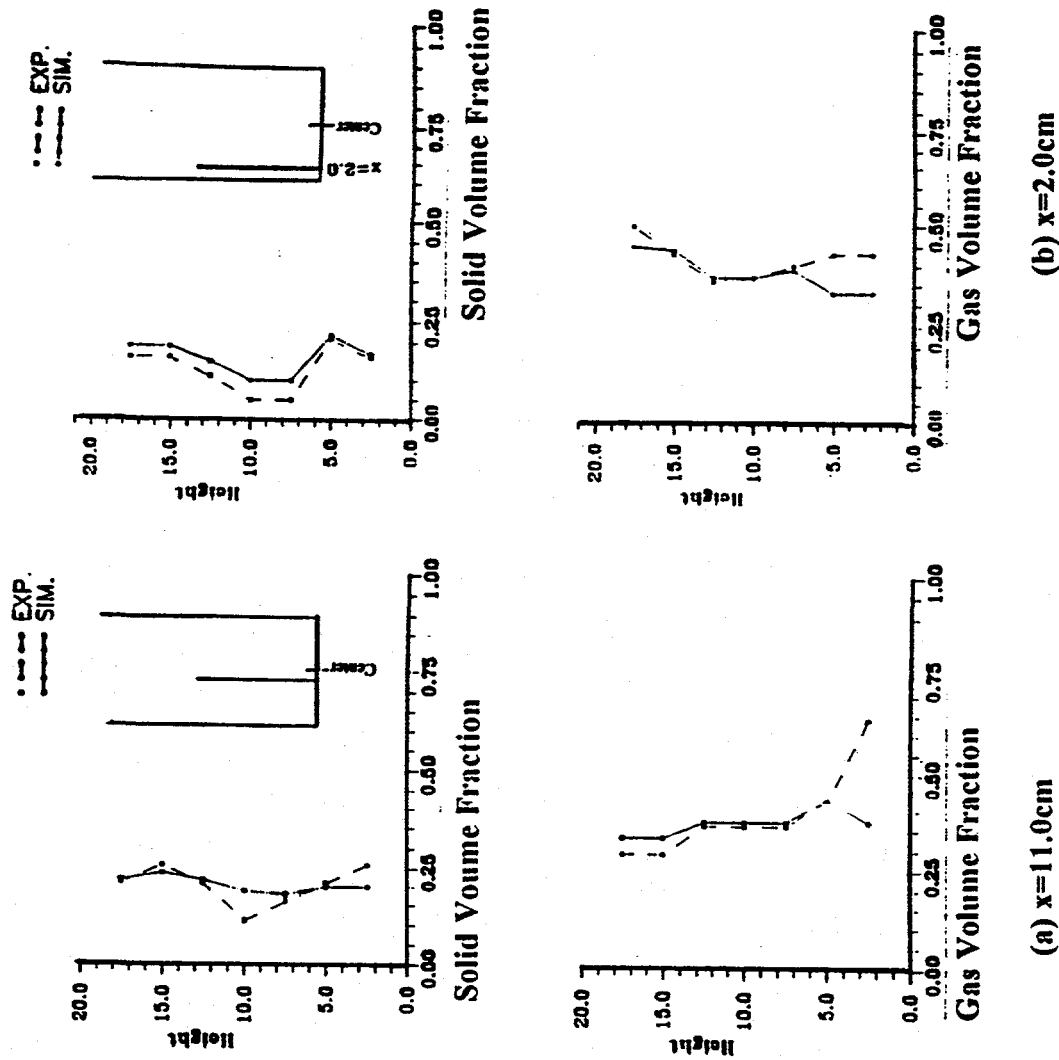
(a) x=11.0cm

(b) x=2.0cm

Figure 5   Comparison of Computed and Experimental Time Average
Volume Fractions at (a) x=11.0cm and (b) x=2.0cm.

Fig. 4 System for Simulation of Three Phase
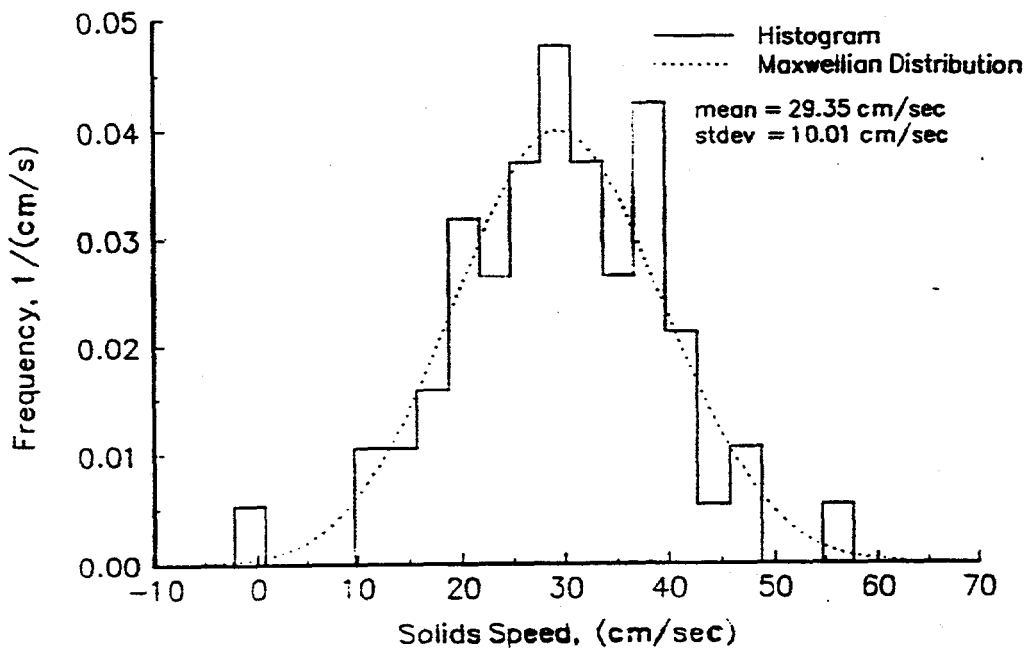Fluidized with Dimensions and Conditions

Fig. 6 Distribution of mean solid speed at x=4 cm and y=4.5 cm for liquid-solid-gas system with V_l=4 cm/s and V_s=3.36 cm/s.

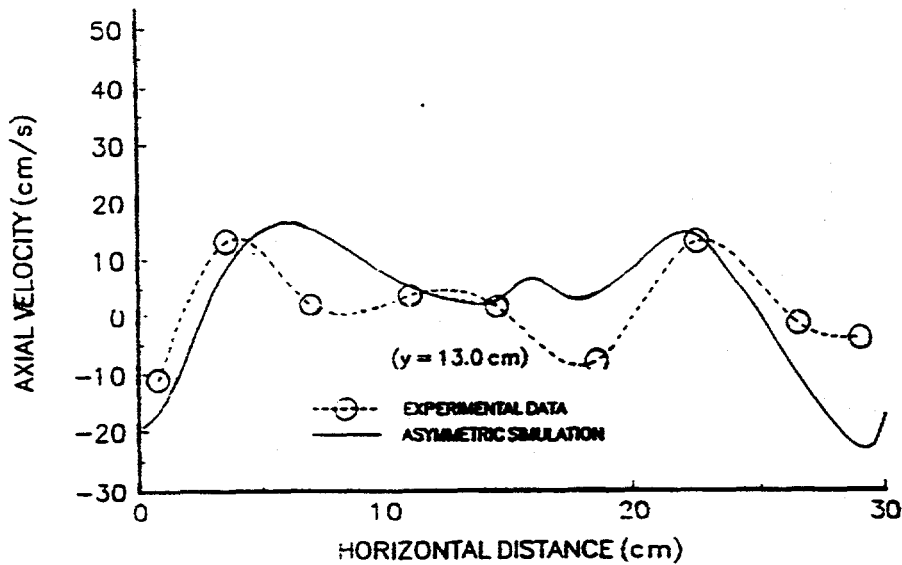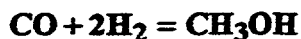**Fig. 7 Comparison of experimental and computed results for solid velocity profile at y=13 cm.**

Table 4 Reaction and Species Balances

$$CO + 2H_2 = CH_3OH$$

Overall rate expression:(Air Products 1992)

$$r = K \cdot f_{CO}^{1/3} \cdot f_{H_2}^{2/3} \left(1 - \frac{f_{MEOH}}{K_{eq} f_{CO} f_{H_2}^2} \right)$$

Mass transfer between gas and liquid:

$$R_i = K_{\ell i} a \left(C_i^{g\ell} - C_i^{\ell} \right)$$

$$K_{\ell i} a = 0.3 \rightarrow 1.3 \quad (1/s) \quad \text{(Ledakowicz 1984 and Viking 1993)}$$

Henry's law and constants (Graaf 1988):

$$C_i^{g\ell} = \frac{f_i}{H_i}$$

$$H_{CO} = 0.175 \exp(638/RT)$$

$$H_{CO_2} = 0.402 \exp(-6947/RT)$$

$$H_{H_2} = 0.0782 \exp(4875/RT)$$

$$H_{CH_3OH} = 1.49 \exp(-17235/RT)$$

Species balance in gas phase:

$$\frac{\partial}{\partial t}(\varepsilon_g \rho_g y_i) + \nabla \cdot (\varepsilon_g \rho_g v_g y_i) = \frac{\alpha_i \varepsilon_s \rho_s M_i r}{3.6 \times 10^6} - \varepsilon_\ell M_i R_i$$

Species balance in liquid phase:

$$\frac{\partial}{\partial t}(\varepsilon_\ell \rho_\ell x_i) + \nabla \cdot (\varepsilon_\ell \rho_\ell v_\ell x_i) = \varepsilon_\ell M_i R_i$$

$$\sum y_i = 1 \qquad \sum x_i = 1$$

$i =$	CO	H_2	CH_3OH	N_2	CO_2
$\alpha_i =$	-1	-2	1	0	0

Table 5 Comparison of IIT's Simulation and LaPorte's RUN E-8.1

	CO Conv. (%)	ε_g gas holdup	slurry height (inches)	total catalyst (kg)	CH$_3$OH (gmol/hr/kg)	net CH$_3$OH (TPD)
Simulation	14.24	26.9	215	740	16.93	9.62
RUN E-8.1	13.50	29.5	200	567	20.50	10.03

GAS (MEOH ...)

The grid is the right
half of the reactor.

22.5"

$\varepsilon_g = 1.000$
$\varepsilon_l = 0.000$
$\varepsilon_s = 0.000$

320"

$\varepsilon_g = 0.050$
$\varepsilon_l = 0.950$
$\varepsilon_s = 0.000$

168"

$\varepsilon_g = 0.050$
$\varepsilon_l = 0.426$
$\varepsilon_s = 0.524$

72"

Syn-Gas
CO   =51%
H_2 =35%
CO_2 =13%
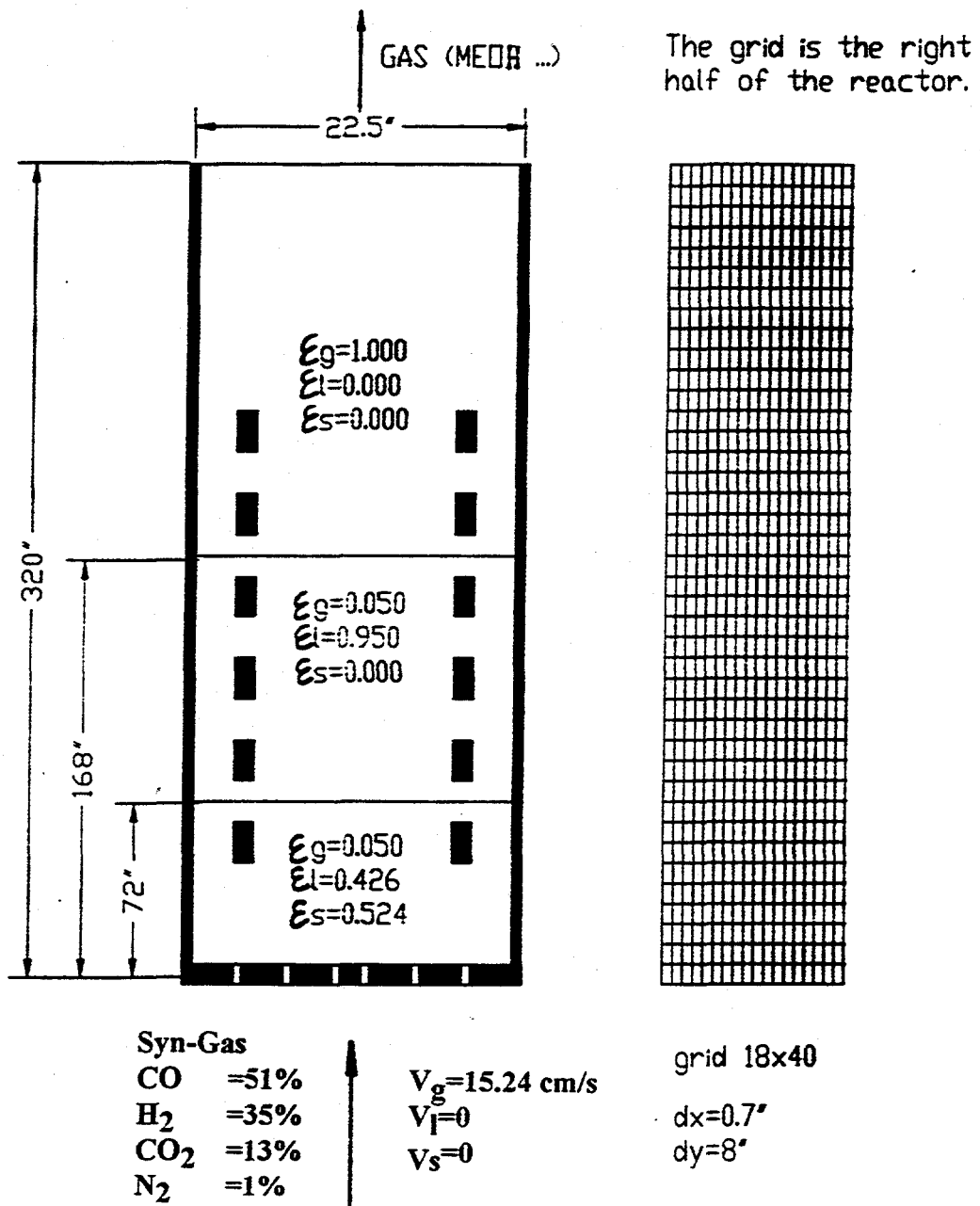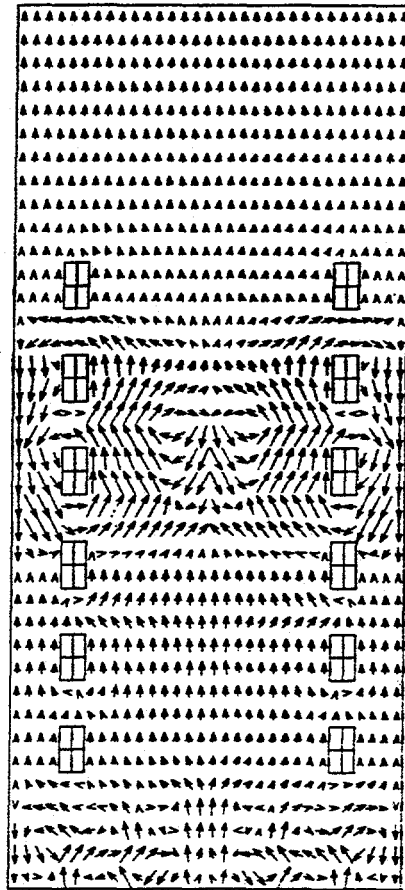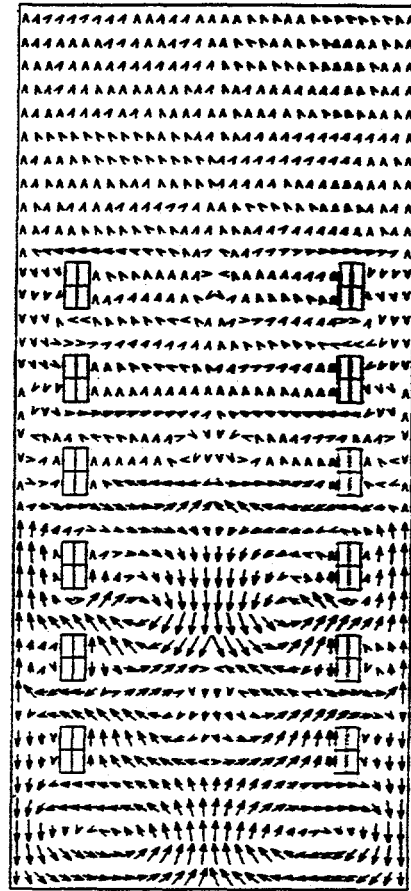N_2 =1%

V_g=15.24 cm/s
V_l=0
V_s=0

grid 18x40

dx=0.7"
dy=8"

Fig. 8 Reactor and Grid with Inlet and Initial Conditions

(P=753.2 psig, T=250.3 °C, $d_p = 50\mu m$, $\rho_s = 3.011\ \frac{g}{cm^3}$, $\rho_\ell = 0.70025\ \frac{g}{cm^3}$)

12

Time = 1 second **Steady State**

Figure 9   Gas Transient Flow Pattern.
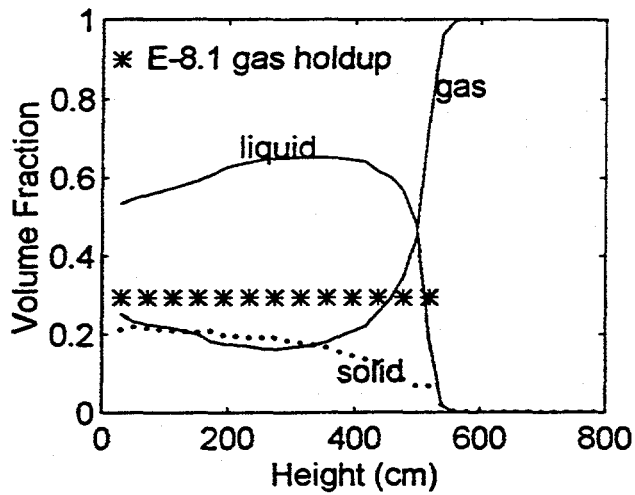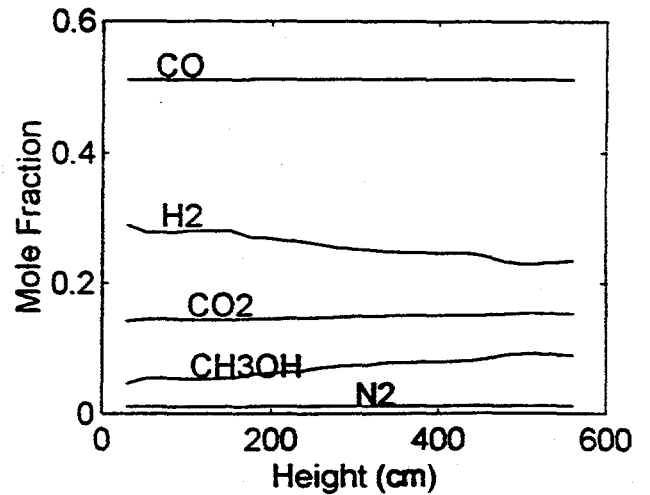

Fig 10 Time average g-l-s volume
fraction profiles

Fig 11 Time average gas
composition profiles

13

NOTATION:

a	interfacial area per unit volume (cm^2/cm^3)
C_i^ℓ	concentration of i in bulk liquid phase
$C_i^{g\ell}$	concentration of i in g-l interface
C_D	drag coefficient
d_k	diameter of solid particle or liquid droplet
e	restitution coefficient
f_i	fugacity of i
H_i	Henry's constant of i
K	reaction kinetic coefficient
K_{eq}	reaction equilibrium constant
$K_{\ell i}$	mass transfer coefficient of i in liquid phase
m_k	rate of generation of phase k
M_i	molecular weight of i
P	pressure
r	rate of reaction
R_i	rate of mass transfer
Re_k	Reynolds number
T	temperature
v	velocity
x_i	weight fraction of i in liquid phase
y_i	weight fraction of i in gas phase

Greek letters:

α_i	stoichimetric coefficient of i
β	frictional coefficient
ε	volume fraction
ρ	density
μ	viscosity
θ	granular temperature
τ	shear stress
ψ	sphericity of particle or droplet

Subscripts:

g, ℓ, s	gas, liquid, solid respectively
i	species
k	solid or liquid phase